AIAA JOURNAL
Vol. 35, No. 5, May 1997

Vibration Suppression Using Acceleration Feedback Control with Multiple Proof-Mass Actuators

Saburo Matunaga,* Yimei Yu,† and Yoshiaki Ohkami‡
Tokyo Institute of Technology, Meguro, Tokyo 152, Japan

The use of direct acceleration feedback control for vibration suppression of low-frequency multi-degree-of-freedom flexible structures using multiple proof-mass actuators is investigated. Considering the effect of actuator dynamics, closed-loop eigenvalue analysis is conducted, and a simple matrix inequality is obtained for the stability condition of the closed-loop system. Methods for calculation of the stability condition are suggested. A procedure for actuator parameter optimization is proposed to assure the closed-loop system performance. Using both a lumped-mass space structure model and a frame structure model, numerical analysis and simulations are performed, and several aspects relating to control design are discussed. The results indicate the effectiveness of acceleration feedback control for low-frequency vibration suppression using proof-mass actuators.

I. Introduction

In the past decade, there has been much research on the use of proof-mass actuators (PMA) as a kind of vibration suppression actuator because it is believed that these actuators can be easily adapted to the space environment. In contrast to many other actuators, whose dynamics are generally neglected during the controller design, PMAs make use of the dynamic coupling of the vibrating structure and the actuator. In Ref. 1, PMA was used conceptually as a passive damper to augment space structure damping and PMA parameter optimization was conducted using a time-domain criteria. A prototype PMA was designed and evaluated in Ref. 2. References 3 and 4 focused on control algorithms, considering the PMA's force and stroke nonlinearity. The problem of structure/actuator/control interaction was discussed in Refs. 5 and 6. In Ref. 5, some sufficient conditions for stability of mechanical systems were given and applied to the case when PMAs were used as vibration suppression actuators. Direct velocity feedback control, or direct displacement feedback control, or a combination of both was adopted as control algorithms. In Ref. 6, local velocity feedback control was discussed, and it was indicated analytically and experimentally that the interaction between the structure, the actuator, and the control algorithm can drive the closed-loop system to instability if the actuator parameters and the feedback gains are not carefully selected. In Ref. 7, passive and active (local velocity feedback) control of PMAs was analyzed experimentally. The instability caused by velocity feedback control was again noticed, and to increase the active vibration suppression effect, the actuator dynamics were carefully determined, which, as a result, were different from that of the passive damper.

In the aforementioned papers, when PMAs have been used for active vibration control of flexible space structures, feedback of absolute structural velocity and/or displacement was employed. However, it is difficult to measure absolute structural velocity or displacement in the space environment due to sensor limitations. In addition, when velocity feedback is involved in the control algorithm, closed-loop stability depends greatly on system parameters such as the frequencies and damping ratios of the structure and the actuators [see Ref. 6, inequalities (6), as an example for a one-degree-of-freedom (DOF) structure]. Thus, it is highly possible that closed-loop instabilities occur when the system is exposed to parameter uncertainties.

Received Aug. 12, 1996; revision received Feb. 8, 1997; accepted for publication Feb. 10, 1997. Copyright © 1997 by the American Institute of Aeronautics and Astronautics, Inc. All rights reserved.

*Research Associate, Department of Mechano-Aerospace Engineering. Member AIAA.
†Ph.D. Student, Department of Mechano-Aerospace Engineering.
‡Professor, Department of Mechano-Aerospace Engineering. Member AIAA.

In this paper, we suggest the use of direct acceleration feedback (DAFB). As opposed to absolute velocity or displacement, it is much easier to measure the acceleration of space structures given available sensors. In addition, as derived later in the paper, a simple closed-form stability condition can be obtained from eigenvalue analysis of DAFB. DAFB has been discussed in Ref. 8 when one active tuned mass damper was attached to a one-DOF model of a building structure. In this paper, we discuss control of multi-degree-of-freedom (MDOF) structures using multiple actuators. The closed-loop stability is analyzed to assist in further understanding of the algorithm. A procedure for actuator parameter optimization is suggested to assure the closed-loop system performance. A lumped-mass low-frequency six-DOF model and a frame structure model are used in numerical analysis and simulations. Results indicate the effectiveness of the proposed algorithm for the suppression of low-frequency vibrations of flexible space structures.

II. System Model and Control Law

In the following, we derive the dynamic equations of the combined system consisting of the main structure and the vibration suppression actuators. Consider a structure described by the n-dimensional second-order vector equations

$$M_s\ddot{\boldsymbol{X}}_s + C_s\dot{\boldsymbol{X}}_s + K_s\boldsymbol{X}_s = \boldsymbol{f}_s \tag{1}$$

where $\boldsymbol{X}_s$ and $\boldsymbol{f}_s$ are, respectively, the structural displacement vector and the external force vector. M_s, C_s, and K_s are, respectively, the structural mass, damping, and stiffness matrices. Suppose M_s is symmetric and positive definite while C_s and K_s are symmetric and either positive definite or positive semidefinite. This model describes an MDOF lumped-mass structure, or it can equally represent a discrete approximation, such as a finite element method (FEM) model, of a complicated space structure. For the sake of convenience, we introduce the modal matrix

$$\Phi = [\phi_1, \phi_2, \ldots, \phi_n] \tag{2}$$

and assume proportional structural damping. Equation (1) can be written in terms of the modal coordinate vector $\boldsymbol{q}$ as follows:

$$I\ddot{\boldsymbol{q}} + 2\Sigma_s\Omega_s\dot{\boldsymbol{q}} + \Omega_s^2\boldsymbol{q} = \Phi^T\boldsymbol{f}_s \tag{3}$$

where

$$\Sigma_s = \mathrm{diag}(\zeta_1, \zeta_2, \ldots, \zeta_n) > 0$$

$$\Omega_s = \mathrm{diag}(\omega_1, \omega_2, \ldots, \omega_n) \geq 0$$

Assume there are m actuators attached to the structure, and introduce X_a as the absolute displacement vector of the actuators. The equations of motion of the combined system can be derived as

$$\begin{bmatrix} I & 0 \\ 0 & M_a \end{bmatrix}\begin{bmatrix} \ddot{q} \\ \ddot{X}_a \end{bmatrix} + \begin{bmatrix} 2\Sigma_s\Omega_s + \Phi^T B C_a B^T \Phi & -\Phi^T B C_a \\ -C_a B^T \Phi & C_a \end{bmatrix}\begin{bmatrix} \dot{q} \\ \dot{X}_a \end{bmatrix} + \begin{bmatrix} \Omega_s^2 + \Phi^T B K_a B^T \Phi & -\Phi^T B K_a \\ -K_a B^T \Phi & K_a \end{bmatrix}\begin{bmatrix} q \\ X_a \end{bmatrix} = \begin{bmatrix} \Phi^T B f_a \\ -f_a \end{bmatrix} \tag{4}$$

where M_a, C_a, and K_a are the m-dimensional mass, damping, and stiffness matrices of the actuators, respectively, and are positive definite and diagonal. The input matrix B contains information relating to the placement of the actuators. The actuator force f_a is a vector, each of whose elements represents a control force generated by an actuator, where the force acts between the actuator's proof mass and the attachment point on the structure.

Assume that for each PMA, there is an acceleration sensor physically collocated with it. The form of DAFB control proposed involves local positive feedback of the sensor output, say, structural accelerations. Under this assumption, f_a becomes

$$f_a = GB^T \Phi \ddot{q} \tag{5}$$

where

$$G = \text{diag}(g_1, g_2, \ldots, g_m) \tag{6}$$

and $g_i \geq 0$ $(i = 1, \ldots, m)$. Because of the low-authority characteristics of the control algorithm, the output of a sensor only affects the output of the actuator collocated with it. This is reflected in the diagonal nature of the feedback gain matrix. Note that a PMA generates force acting between the proof mass and the attachment point on the structure, while the accelerations in the algorithm are absolute accelerations of the structure. Therefore, although the sensors and the actuators are physically collocated, the control algorithm is essentially a noncollocated feedback control.

III. Closed-Loop Eigenvalue Analysis

From eigenvalue analysis, a closed-loop stability condition is obtained for the DAFB control algorithm. Methods for the calculation of the stability condition are then proposed.

Closed-Loop Stability Condition

Theorem: The elastic vibrations of the closed-loop system are asymptotically stable if the following matrix inequality holds:

$$I - \Phi^T B G B^T \Phi > 0 \tag{7}$$

Proof: Applying a congruence transformation to Eq. (4),

$$\begin{bmatrix} q \\ X_r \end{bmatrix} = \begin{bmatrix} I & 0 \\ -B^T\Phi & I \end{bmatrix}\begin{bmatrix} q \\ X_a \end{bmatrix} \tag{8}$$

where X_r is the vector of the relative displacement between the actuator proof mass and the structure, we get

$$\begin{bmatrix} I + \Phi^T B M_a B^T \Phi & \Phi^T B M_a \\ M_a B^T \Phi & M_a \end{bmatrix}\begin{bmatrix} \ddot{q} \\ \ddot{X}_r \end{bmatrix} + \begin{bmatrix} 2\Sigma_s\Omega_s & 0 \\ 0 & C_a \end{bmatrix}\begin{bmatrix} \dot{q} \\ \dot{X}_r \end{bmatrix} + \begin{bmatrix} \Omega_s^2 & 0 \\ 0 & K_a \end{bmatrix}\begin{bmatrix} q \\ X_r \end{bmatrix} = \begin{bmatrix} 0 \\ -f_a \end{bmatrix} \tag{9}$$

From Eq. (5), the closed-loop equation becomes

$$\begin{bmatrix} I + \Phi^T B M_a B^T \Phi & \Phi^T B M_a \\ (M_a + G) B^T \Phi & M_a \end{bmatrix}\begin{bmatrix} \ddot{q} \\ \ddot{X}_r \end{bmatrix} + \begin{bmatrix} 2\Sigma_s\Omega_s & 0 \\ 0 & C_a \end{bmatrix}\begin{bmatrix} \dot{q} \\ \dot{X}_r \end{bmatrix} + \begin{bmatrix} \Omega_s^2 & 0 \\ 0 & K_a \end{bmatrix}\begin{bmatrix} q \\ X_r \end{bmatrix} = \begin{bmatrix} 0 \\ 0 \end{bmatrix} \tag{10}$$

Through a similar transformation (note that $M_a > 0$ and $G \geq 0$),

$$\begin{bmatrix} q \\ X_r \end{bmatrix} = \begin{bmatrix} I & 0 \\ 0 & M_a^{-\frac{1}{2}}(M_a + G)^{\frac{1}{2}} \end{bmatrix}\begin{bmatrix} q \\ \tilde{X}_r \end{bmatrix} \tag{11}$$

and making use of the commutability property of the diagonal matrices (notice that M_a and G are both diagonal), we obtain the following symmetrized closed-loop equation:

$$\begin{bmatrix} I + \Phi^T B M_a B^T \Phi & \Phi^T B M_a^{\frac{1}{2}}(M_a + G)^{\frac{1}{2}} \\ (M_a + G)^{\frac{1}{2}} M_a^{\frac{1}{2}} B^T \Phi & M_a \end{bmatrix}\begin{bmatrix} \ddot{q} \\ \ddot{\tilde{X}}_r \end{bmatrix} + \begin{bmatrix} 2\Sigma_s\Omega_s & 0 \\ 0 & C_a \end{bmatrix}\begin{bmatrix} \dot{q} \\ \dot{\tilde{X}}_r \end{bmatrix} + \begin{bmatrix} \Omega_s^2 & 0 \\ 0 & K_a \end{bmatrix}\begin{bmatrix} q \\ \tilde{X}_r \end{bmatrix} = \begin{bmatrix} 0 \\ 0 \end{bmatrix} \tag{12}$$

For the sake of convenience, we rewrite Eq. (12) as

$$\hat{M}\ddot{Y} + \hat{C}\dot{Y} + \hat{K}Y = 0 \tag{13}$$

where the definitions of the new variables are clear. Consider the eigenvalue problem of Eq. (13),

$$(\hat{M}s^2 + \hat{C}s + \hat{K})\nu = 0 \tag{14}$$

where s is an eigenvalue and $\nu \neq 0$ is its corresponding eigenvector. Premultiplying Eq. (14) by ν^T, we have

$$\hat{m}s^2 + \hat{c}s + \hat{k} = 0 \tag{15}$$

where the following scalars are defined:

$$\hat{m} = \nu^T \hat{M} \nu; \qquad \hat{c} = \nu^T \hat{C} \nu; \qquad \hat{k} = \nu^T \hat{K} \nu \tag{16}$$

Now consider the following two cases: 1) the structure does not have a rigid mode, that is, $\Omega_s > 0$, and 2) the structure has rigid modes, that is, $\Omega_s \geq 0$. In case 1, referring to Eq. (12), we have $\hat{C} > 0$ and $\hat{K} > 0$, which implies $\hat{c} > 0$ and $\hat{k} > 0$. Thus, if the mass matrix $\hat{M}$ is also positive definite, we will have $\hat{m} > 0$, and accordingly all of the roots of Eq. (15) will have a negative real part, which implies asymptotical stability of the closed-loop system. In case 2, we have $\hat{C} \geq 0$ and $\hat{K} \geq 0$. From the structure of $\hat{C}$ and $\hat{K}$, it can be verified that, for Eq. (15), either $\hat{c} > 0$ and $\hat{k} > 0$ or $\hat{c} = 0$ and $\hat{k} = 0$, where the former corresponds to the elastic vibration modes and the latter corresponds to the rigid modes. Thus, if $\hat{M}$ is positive definite and accordingly $\hat{m} > 0$, the nonzero roots of Eq. (15) will lie in the open left-half plane. Therefore, for both cases 1 and 2, the elastic vibrations of the closed-loop system are asymptotically stable if $\hat{M} > 0$.

Consider the following bilinear form whose positive definiteness is equivalent to that of $\hat{M}$:

$$V = \begin{bmatrix} y_1 \\ y_2 \end{bmatrix}^T \begin{bmatrix} I + \Phi^T B M_a B^T \Phi & \Phi^T B M_a^{\frac{1}{2}}(M_a + G)^{\frac{1}{2}} \\ (M_a + G)^{\frac{1}{2}} M_a^{\frac{1}{2}} B^T \Phi & M_a \end{bmatrix}\begin{bmatrix} y_1 \\ y_2 \end{bmatrix} \tag{17}$$

where $y = [y_1^T, y_2^T]^T$ is an arbitrary vector. Then after some manipulation, we get

$$V = y_1^T (I - \Phi^T B G B^T \Phi) y_1 + \left| (M_a + G)^{\frac{1}{2}} B^T \Phi y_1 + M_a^{\frac{1}{2}} y_2 \right|^2 \tag{18}$$

whose positive definiteness is equivalent to the inequality (7). □

The closed-loop stability condition given by inequality (7) provides a constraint on the feedback gain matrix. To help further understand this, we rewrite the inequality in an equivalent form as follows. Recalling that $\Phi^T M_s \Phi = I$, we have

$$\Phi^T (M_s - BGB^T)\Phi > 0 \tag{19}$$

or, consequently,

$$M_s - BGB^T > 0 \tag{20}$$

Thus, the stability condition depends only on the mass distribution of the structure, placement of the actuators, and the magnitude of the feedback gain. This is a simple condition and is rather robust to parameter change.

Calculation of Stability Condition

In this section we consider the calculation of the stability condition in the m-dimensional gain vector space:

$$\Xi: \boldsymbol{g} = (g_1, g_2, \ldots, g_m)^T \in R_+^m \tag{21}$$

where the subscript + implies the nonnegativeness of g_i ($i = 1, \ldots, m$). Moreover, assume that the set of all gain vectors satisfying closed-loop stability is

$$\tilde{\Xi} = \{\boldsymbol{g} \in \Xi \mid \text{closed-loop stable}\} \tag{22}$$

Expanding inequality (7), we obtain

$$g_1 \Phi^T B_1 B_1^T \Phi + g_2 \Phi^T B_2 B_2^T \Phi + \cdots + g_m \Phi^T B_m B_m^T \Phi < I \tag{23}$$

or

$$g_1 U_1 + g_2 U_2 + \cdots + g_m U_m < 1 \tag{24}$$

where B_i ($i = 1, \ldots, m$) are the columns of the placement matrix B and the definition of the U_i is clear. Inequality (24) requires that

$$\lambda_{\max}(g_1 U_1 + g_2 U_2 + \cdots + g_m U_m) < 1 \tag{25}$$

where $\lambda_{\max}$ is a real scalar function defined on a real symmetric matrix and whose value represents the maximum eigenvalue of the matrix. Consider a direction cosine vector

$$\boldsymbol{i} = (\cos\theta_1, \cos\theta_2, \ldots, \cos\theta_m)^T \tag{26}$$

in the gain vector space, and assume $\boldsymbol{g} = r\boldsymbol{i}$ is a vector along this direction, that is, $g_i = r\cos\theta_i$ ($i = 1, \ldots, m$). To satisfy the stability condition (25), r must satisfy

$$r < r_{\sup} = \lambda_{\max}^{-1}(\cos\theta_1 U_1 + \cos\theta_2 U_2 + \cdots + \cos\theta_m U_m) \tag{27}$$

Actually, $r_{\sup}$ is a function of the direction, that is, $r_{\sup} = r_{\sup}(\boldsymbol{i})$, and $\tilde{\Xi}$ is the volume covered by the surface $r_{\sup}(\boldsymbol{i})$ when $\boldsymbol{i}$ spans all of the admissible directions (the directions that satisfy $g_i \geq 0$).

In the following, we suggest a simple method for calculating $\tilde{\Xi}$. We approximate $\tilde{\Xi}$ by a region that can be described by a set of inequalities decoupled in each of the feedback gains:

$$\{\boldsymbol{g} \in \Xi \mid 0 \leq g_i < (1-\alpha) r_{0i},\ (i = 1, \ldots, m)\} \tag{28}$$

where $r_{0i} = r_{\sup}(\boldsymbol{e}_i)$ and $\boldsymbol{e}_i$ is a unit vector along the direction of the ith coordinate axis:

$$\boldsymbol{e}_i = (0, \ldots, 0, \overset{i}{\check{1}}, 0, \ldots, 0)^T$$

Another parameter in Eq. (28), $\alpha \in [0, 1)$, can be determined through calculation along the direction $(r_{01}, r_{02}, \ldots, r_{0m})^T$. Figure 1 illustrates the principle of the simplified method for a two actuator case with the shaded rectangular area approximating the stability region. This method was applied to several different structure models, and in each case, $\tilde{\Xi}$ could be approximated with a small α. The stability region in the gain vector space calculated by the simplified method is somewhat smaller than the exact one, but because, for the sake of robustness, we do not usually select feedback gains too close to the unstable region, this approximation is acceptable.

IV. Example of Low-Frequency Control

In this section we apply the control algorithm to two low-frequency flexible structure models: a six-DOF lumped-mass model and a plane frame structure model. Aspects relating to control design are discussed.

Table 1 Structural modal information

Frequency, rad/s	Eigenvalue real part	Damping ratio, %
0	0	——
1.6659	−0.0033	0.2
2.7688	−0.0055	0.2
4.5052	−0.0090	0.2
6.7911	−0.0136	0.2
10.1348	−0.0203	0.2

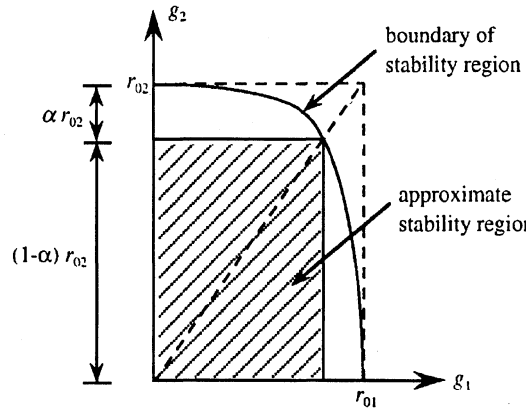

Fig. 1 Approximation of the stability region.

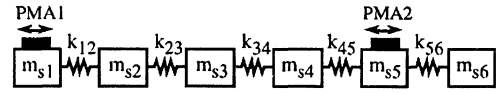

Fig. 2 Lumped-mass six-DOF space structure model and placement of actuators.

Six-DOF Lumped-Mass Model

Modeling

Figure 2 shows a schematic of the low-frequency six-DOF lumped-mass model used in the numerical analysis and simulation. The physical parameters of the structure (with m_s in kilograms and k in newtons per meter) are as follows:

$$m_{s1} = 2.0, \quad m_{s2} = 1.4, \quad m_{s3} = 1.0$$

$$m_{s4} = 1.0, \quad m_{s5} = 1.4, \quad m_{s6} = 2.0$$

$$k_{12} = 9, \quad k_{23} = 25, \quad k_{34} = 36$$

$$k_{45} = 25, \quad k_{56} = 9$$

For the sake of convenience, the inherent damping in the structure is not shown in Fig. 2 but is assumed to be proportional with a modal damping ratio of 0.002. Table 1 gives the relevant modal information for the structure.

Suppose we use two actuators to control the vibrations of the structure. The spring constant and the damping ratio of the PMAs are assumed to be tunable, and the mass of each actuator is fixed at 0.1 kg. The ratio of the total mass of the actuators to the mass of the structure is 2.27%.

Actuator Placement

The placement of the actuators is determined by the relative importance and shape of each mode. Let us choose the elastic deformation of the structure as the variable of interest. Using component cost analysis[9] and assuming that each mass element of the structure is exposed to a disturbance, the relative importance of the elastic modes can be calculated as 65.95, 24.23, 6.19, 2.60, and 1.03%. Thus, the first and second modes are the most important ones.

Investigation into the mode shape of these elastic modes shows that the first and second modes are most controllable when the actuators are attached to the end-mass elements.[10] However, in this case,

the third, fourth, and fifth elastic modes will be almost uncontrollable. To impose some active control influence on these higher-order modes, we attach the actuators as shown in Fig. 2.

Control Parameter Determination

For DAFB control design, the control parameters that need to be determined include the feedback gains and the physical parameters of the actuators. The feedback gains are determined by trial and error, and the actuator parameters are determined by optimization. For optimization of actuator (especially passive damper) parameters, the two criteria most often used are the Den Hartog frequency domain criterion[11] and the time-domain criterion.[1] The former minimizes the maximum value of the transmissibility of the combined system, and the latter minimizes a time-domain quadratic performance index. The selection of an appropriate optimization criterion is problem dependent. In this paper, an eigenvalue optimization criterion is adopted, because the damping is determined by the system eigenvalues, and such a criterion can be easily applied to control of MDOF structures with multiple actuators. For the simplest case when one actuator is attached to a one-DOF structure, the optimization criterion can be written as follows. Assuming the closed-loop eigenvalues are s_i $(i = 1, \ldots, 4)$, optimize the actuator parameters so that σ is maximized, where

$$\sigma = \min_i[-\mathrm{Re}(s_i)]$$

For the same feedback gains, by optimization of actuator parameters, the closed-loop system eigenvalues are located as far into the left half plane as possible. For the case when multiple actuators are attached to an MDOF structure, the same criterion is applied to each target mode and its control actuator. In other words, between the two pairs of conjugate eigenvalues representing the structure dominated mode (target mode) and the actuator dominated mode, the pair closer to the imaginary axis is moved as far into the left-half plane as possible.

Once the feedback gains, $g_i \geq 0$ $(i = 1, \ldots, m)$, have been selected, the following one actuator at a time procedure is adopted for optimizing the actuator parameters: 1) set the actuator parameters to their initial values,

$$\omega_{ai} = \omega_{ai0}, \qquad \zeta_{ai} = \zeta_{ai0} \qquad (i = 1, \ldots, m)$$

2) $i = 1$; 3) retaining the parameter values for the other PMAs, optimize the frequency and damping ratio of PMAi with respect to its target mode and the initial values ω_{ai} and ζ_{ai}, using the eigenvalue criterion (assume the resultant optimum parameters are, respectively, ω_{opt} and ζ_{opt}); 4) $\omega_{ai} = \omega_{\mathrm{opt}}$ and $\zeta_{ai} = \zeta_{\mathrm{opt}}$; 5) if $i < m$, $i = i + 1$, and go to step 3, otherwise, go to step 6; and 6) go to step 2 unless the actuator parameters ω_{ai} and ζ_{ai} $(i = 1, \ldots, m)$ converge.

Note that the phrase initial values in steps 1 and 3 refers to different things. In step 1, it refers to the initial values for the whole procedure, whereas in step 3, it refers to those for the optimization carried out in that step. The convergence of this procedure depends on the selection of the initial values in step 1. This issue will be discussed later.

After the actuator parameters have been optimized, the eigenvalues of the closed-loop system are calculated, and simulations are conducted to see if the requirements on closed-loop damping and stroke length are satisfied (as an example, for stroke length we can require that it not exceed the stroke limit for the initial conditions corresponding to the worst disturbance). If the requirements are not satisfied, the feedback gains should be adjusted. This is done by trial and error. Given that the feedback gains satisfy the stability condition, the larger the feedback gain, the larger the closed-loop damping and the stroke length are.

Optimal Passive Tuning

We first consider the case when the PMAs are used as passive vibration absorbers. The results will be later compared with those for acceleration feedback.

For the six-DOF lumped-mass structure shown in Fig. 2, PMA1 (attached to m_{s1}) is tuned optimally to the first mode, whereas PMA2 (attached to m_{s5}) is tuned to the second mode. After setting the feedback gains to zero, the optimization procedure proposed before is used to determine the actuator parameters. Consider the selection

Table 2 Modes of the combined system under passive optimal control

	Frequency, rad/s	Eigenvalue real part	Damping ratio, %
Rigid mode	0	0	—
1st, a[a]	1.6365	−0.1267	7.72
1st, s[b]	1.6400	−0.1268	7.71
2nd, a	2.7599	−0.1244	4.50
2nd, s	2.7688	−0.1242	4.48
3rd, s	4.5433	−0.0276	0.61
4th, s	6.8026	−0.0199	0.29
5th, s	10.1357	−0.0210	0.21

[a]Actuator. [b]Structure.

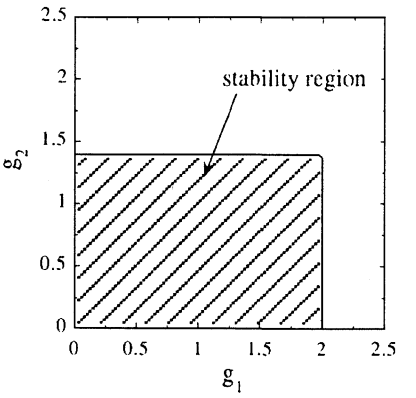

Fig. 3 Gain region satisfying the stability conditions.

of the initial value for the actuator parameters (step 1 of the procedure). The initial frequency for each actuator is set to that of its target mode, and regarding initial damping ratios, for this example, the procedure converges when they lie in the range from 0.01 to 0.78. That is, it is easy to choose initial values that ensure that the procedure converges. The resultant optimal parameters of the actuators are

$$\omega_{a1} = 1.6206, \qquad \omega_{a2} = 2.7629$$

$$\zeta_{a1} = 0.1516, \qquad \zeta_{a2} = 0.0881$$

and the resulting eigenvalue information of the combined system is given in Table 2. Referring to Table 1, it can be seen that optimal passive control adds damping to the object modes, whereas the nonobject modes are left almost unimproved.

Acceleration Feedback

For this example, the stability region in the two-dimensional gain vector space is calculated and indicated in Fig. 3. Using the simplified method, this region can be approximated by

$$0 \leq g_1 < 2, \qquad 0 \leq g_2 < 1.4$$

with $\alpha \approx 0$. For this example, the simplified method gives a very close approximation because there is only slight interaction between the two PMAs.

We first consider the case when PMA1 is used actively and PMA2 optimal passively. The feedback gain for PMA1 is chosen as 0.3, so that the closed-loop damping for the first mode is about twice that of the optimal passive case. This gain is well under the stability gain limit and, thus, the system is safe in the presence of reasonable structural uncertainties. When applying the optimization procedure, the initial value for the actuator parameters are set to the optimal passive ones. The resultant optimal parameters are

$$\omega_{a1} = 1.5481, \qquad \omega_{a2} = 2.8246$$

$$\zeta_{a1} = 0.3058, \qquad \zeta_{a2} = 0.1134$$

Note that for PMA1, the optimum frequency is slightly smaller than and the optimum damping ratio is about twice that of the passive

Table 3 Modes of the closed system with PMA1 used actively and PMA2 used optimal passively

	Frequency, rad/s	Eigenvalue real part	Damping ratio, %
Rigid mode	0	0	—
1st, a[a]	1.6133	−0.2590	15.85
1st, s[b]	1.6411	−0.2589	15.59
2nd, a	2.8242	−0.1891	6.68
2nd, s	2.8296	−0.1888	6.66
3rd, s	4.5642	−0.0408	0.89
4th, s	6.8054	−0.0226	0.33
5th, s	10.1358	−0.0212	0.21

[a]Actuator. [b]Structure.

Table 4 Modes of the closed-loop system with both actuators used actively

	Frequency, rad/s	Eigenvalue real part	Damping ratio, %
Rigid mode	0	0	—
1st, a[a]	1.5999	−0.2605	16.07
1st, s[b]	1.6459	−0.2604	15.63
2nd, a	2.8111	−0.3022	10.69
2nd, s	2.8295	−0.3022	10.62
3rd, s	4.8613	−0.1734	3.57
4th, s	7.0899	−0.1215	1.71
5th, s	10.1915	−0.0341	0.33

[a]Actuator. [b]Structure.

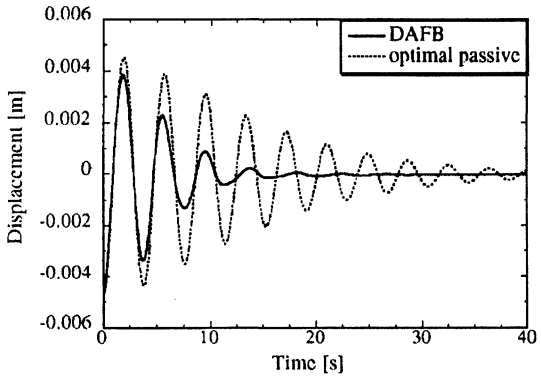

Fig. 4 Initial displacement response of lumped-mass structure.

case. For PMA2, which is used passively, the optimum parameters also changed because of the influence of PMA1. The closed-loop eigenvalues are given in Table 3. Comparing the results in Table 3 with those of Table 2, we can see that the damping ratio of the first pair of modes in Table 3 is twice that of the optimal passive case, as expected, and in addition, damping of the second pair of modes is also improved. Figure 4 shows the displacement of m_{s1} when the structure undergoes an initial displacement caused by a harmonic excitation at the frequency of the first elastic mode. The optimal passive results are shown alongside for comparison. The results indicate much faster damping under acceleration feedback control than under optimal passive control. In terms of the maximum stroke length of PMA1, the value for active control is 2.45 times that for passive control. This is considered tolerable for this example.

Table 4 gives the closed-loop eigenvalue information for the case when both actuators are used actively. The value of both gains is 0.3. With the initial values set to the optimal passive ones, the optimal actuator parameters are calculated as

$$\omega_{a1} = 1.5428, \qquad \omega_{a2} = 2.7977$$

$$\zeta_{a1} = 0.3069, \qquad \zeta_{a2} = 0.2136$$

Note that the optimal damping for PMA2 is almost twice that for the passive case. Referring to Table 4, we can see that the first and second pairs of modes are highly damped, and damping of the third and

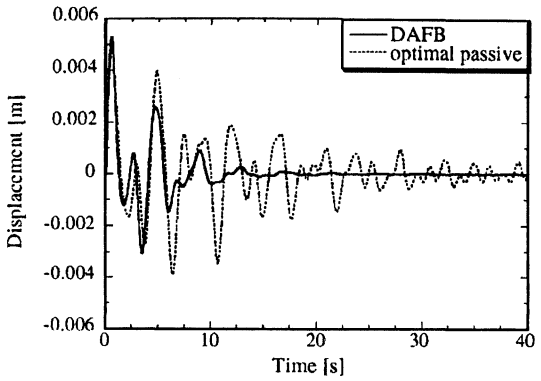

Fig. 5 Impulse response of lumped-mass structure.

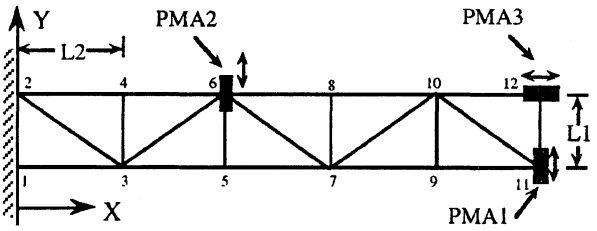

Fig. 6 Plane frame structure model and placement of actuators.

fourth structural modes is also improved to some extent. Damping of the last structural mode improved only a little, but because the relative importance of this mode is only 1.03%, we can expect that it will only slightly influence our variable of interest, the structural deformation.

Figure 5 shows the displacement response of m_{s1} when the structure is subject to two impulses of the same magnitude but opposite in direction and acting, respectively, on m_{s1} and m_{s2}. In this case, all of the elastic modes are excited and the rigid modes are not. It can be seen that as a kind of active control, DAFB control is much more effective than passive control for damping out the vibrations.

Compared with optimal passive control, for the same structure initial conditions, optimal DAFB control dissipates vibration energy much faster through larger proof-mass stroke and larger actuator damping. Similar to local velocity feedback control in Refs. 6 and 7, damping in the actuator dominated mode is decreased to increase the damping of the structure dominated mode. However, for velocity feedback control, the actuator frequency of each PMA has to be below all of the structural modes to avoid instabilities, whereas for DAFB control, the actuator frequencies are not necessarily below all of the structural modes, for example, in the case of PMA2 in the preceding example.

Plane Frame Structure

Modeling

The model we use is the plane frame structure shown in Fig. 6 with $L_1 = 2.4$ m and $L_2 = 3.0$ m. The frame elements are connected rigidly. Assume each element has a mass density of 21.206 kg/m, a flexural rigidity EI of 2.036×10^3 Nm^2, and an extensional rigidity EA of 1.414×10^5 N. The structure is modeled using finite element analysis. The full-order FEM model has 30 modes, but during simulations we use a reduced 11th-order model since, in general, the high-order modes are only minimally excited. The mode shapes for the first five modes are shown in Fig. 7, and the corresponding natural frequencies are given alongside. It can be seen clearly that the third mode is dominated by longitudinal vibrations and the other four modes are dominated by bending vibrations. For modes above the fifth mode, this kind of domination is not obvious, and for higher modes, the mode shape is twisted because the bending effect for each single element becomes strong. The modal damping ratio matrix for the first 11 modes is assumed to be as follows: diag(0.005, 0.005, 0.005, 0.01, 0.03, 0.03, 0.03, 0.03, 0.03, 0.03, 0.03).

Table 5 Comparison of the closed-loop eigenvalues under passive and active control

	Passive	Active
1st, a[a]	$-0.0759 \pm 0.9213i$	$-0.1474 \pm 0.9084i$
1st, s[b]	$-0.0758 \pm 0.9281i$	$-0.1473 \pm 0.9226i$
2nd, a	$-0.2351 \pm 3.8772i$	$-0.6394 \pm 3.8795i$
2nd, s	$-0.2351 \pm 3.8894i$	$-0.6397 \pm 3.8925i$
3rd, a	$-0.3499 \pm 5.9822i$	$-1.0103 \pm 5.9584i$
3rd, s	$-0.3499 \pm 5.9989i$	$-1.0103 \pm 6.0328i$
4th, s	$-0.0941 \pm 7.9509i$	$-0.3839 \pm 8.3033i$
5th, s	$-0.3250 \pm 10.7718i$	$-0.3622 \pm 10.9188i$

[a]Actuator. [b]Structure.

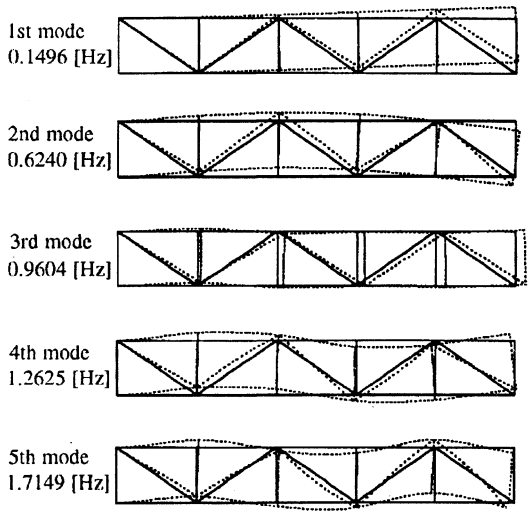

Fig. 7 Modal shapes and natural frequencies of the frame structure.

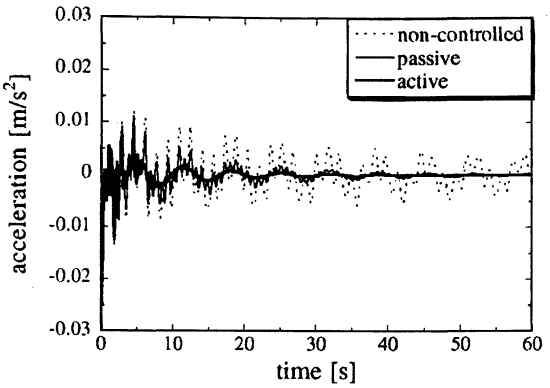

At joint 11 along *Y* axis

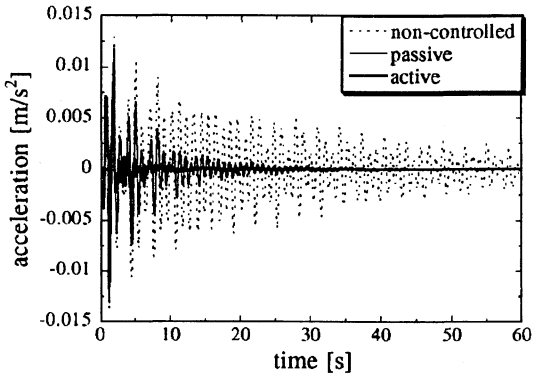

At joint 12 along *X* axis

Fig. 8 Acceleration impulse response of the frame structure.

Actuator Placement

Suppose we use three actuators to control the first three modes, which are assumed to be the most important. Referring to the mode shapes in Fig. 7, we locate the actuators as shown in Fig. 6 with the actuator number corresponding to the target mode, so that these modes are most controllable. The actuators are all of the same mass, and the ratio of the total mass of the actuators to the mass of the structure is assumed to be 2.08%.

Numerical Results

Parameter design for optimal passive control and acceleration feedback control was carried out following the aforementioned procedure. Considering the actuator stroke limitations, the feedback gain vector for acceleration feedback control is selected to be $(56, 25, 72)^T$, which is well under the stability gain limit $(219.7, 137.5, 377.5)^T$ calculated by the simplified method mentioned earlier. A comparison of the eigenvalues for the optimal passive and acceleration feedback control is given in Table 5. Compared with optimal passive control, acceleration feedback control adds more than twice the damping to the target modes, and it also adds large damping to the fourth mode even though this mode is not included among the target modes.

Figure 8 shows the acceleration responses of the frame structure at joint 11 along the Y axis and at joint 12 along the X axis, for the open-loop, passive, and active control cases when the system is subject to an impulse acting on joint 12 with a direction angle of $\pi/3$. Referring to the simulation results, passive control can damp the structural vibrations rather effectively, but acceleration feedback control gives more effective results when faster damping is required. Besides impulse responses, the response of the system to random disturbances with low cut-off frequencies was investigated, and the effectiveness of acceleration feedback control was again verified.

Compared with other kinds of sensor output, acceleration outputs contain more high-frequency vibration modes, and are more easily affected by high-frequency noises. When high-frequency components dominate the sensor output, the efficiency of the DAFB control over low-frequency modes will be reduced, although, theoretically, no instability will occur. This matter needs further investigation.

V. Conclusions

This paper investigated the use of direct acceleration feedback control for vibration suppression of low-frequency MDOF space structures using multiple PMAs. A general closed-loop eigenvalue analysis was conducted, and a stability condition [Eq. (7)] was derived as a constraint on the feedback gain matrix. Methods for the calculation of the stability constraint on the feedback gains were discussed. Several aspects relating to control design were discussed, and an optimization procedure for actuator parameters was proposed. Numerical analysis and simulations of acceleration feedback control were conducted for a low-frequency six-DOF lumped-mass space structure model and a frame structure model. The results were compared with those for optimal passive control. Simulation results demonstrate the effectiveness of the proposed algorithm.

References

[1]Juang, J.-N., "Optimal Design of a Passive Vibration Absorber for a Truss Beam," *Journal of Guidance, Control, and Dynamics*, Vol. 7, No. 6, 1984, pp. 733–739.

[2]Zimmerman, D. C., Horner, G. C., and Inman, D. J., "Microprocessor Controlled Force Actuator," *Journal of Guidance, Control, and Dynamics*, Vol. 11, No. 3, 1988, pp. 230–236.

[3]Politansky, H., and Pilkey, W. D., "Suboptimal Feedback Vibration Control of a Beam with a Proof-Mass Actuator," *Journal of Guidance, Control, and Dynamics*, Vol. 12, No. 5, 1989, pp. 691–697.

[4]Lindner, D. K., Celano, T. P., and Ide, E. N., "Vibration Suppression Using a Proof-Mass Actuator Operating in Stroke/Force Saturation," *Journal of Vibration and Acoustics*, Vol. 113, Oct. 1991, pp. 423–433.

[5]Inman, D. J., "Control/Structure Interaction: Effects of Actuator Dynamics," *Mechanics and Control of Large Flexible Structures*, edited by J. L. Junkins, Vol. 129, Progress in Astronautics and Aeronautics, AIAA, Washington, DC, 1990, pp. 507–533.

[6]Zimmerman, D. C., and Inman, D. J., "On the Nature of the Interaction Between Structures and Proof-Mass Actuators," *Journal of Guidance, Control, and Dynamics*, Vol. 13, No. 1, 1990, pp. 82–88.

[7]Garcia, E., Webb, S., and Duke, J., "Passive and Active Control of a Complex Flexible Structure Using Reaction Mass Actuators," *Journal of Vibration and Acoustics*, Vol. 117, Jan. 1995, pp. 116–122.

[8]Nishimura, I., Sakamoto, M., Yamada, T., Koshika, N., and Kobori, T., "The Optimal Active Tuned Mass Damper Under Random Excitation," *Fifth International Conference on Adaptive Structures*, Technomic, Lancaster, PA, 1995, pp. 334–343.

[9]Skelton, R. E., *Dynamic Systems Control: Linear Systems Analysis and Synthesis*, Wiley, New York, 1988, Chap. 4.

[10]Yang, B., "Modal Controllability and Observability of General Mechanical Systems," *Journal of Vibration and Acoustics*, Vol. 117, Oct. 1995, pp. 510–515.

[11]Den Hartog, J. P., *Mechanical Vibrations*, Dover, New York, 1985, pp. 93–106.

A. Berman
Associate Editor